CHAPTER IV
RESULTS AND DISCUSSION

4.1 Cultivation of Bacterial Cellulose

Bacterial cellulose sheets were produced from *Acetobacter xylinum,* which was statically inoculated in a suitable culture medium at 30 °C, for 4 days as shown in Figure 4.1.

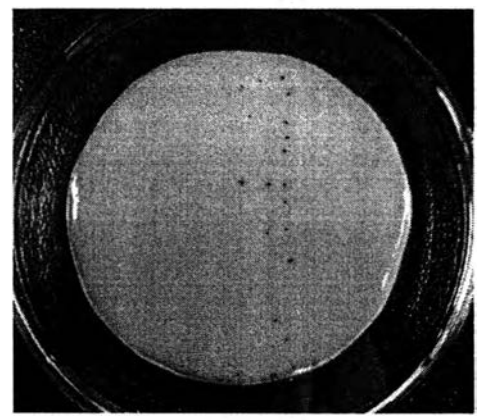

Figure 4.1 Cultivation of *Acetobacter xylinum* under statically conditions in the forming of the white pellicle bacterial cellulose.

In static conditions, *Acetobacter xylinum* produced cellulose sheets on the surface of nutrient broth, at the oxygen-rich air-liquid interface. The subfibrils of cellulose were continuously extruded from linearly ordered pores at the surface of the bacterial cell, crystallized into microfibrils, and forced deeper into the growth medium. During growth and production of bacterial cellulose, the bacterial cells were gradually entrapped in the pellicle. It is a generally accepted that bacterial cellulose which synthesized by a highly aerobic *Acetobacter xylinum* can help the bacterial cells to float and reach the oxygen-rich surface. As a result, the bacterial cellulose was formed at the air-liquid interface of culture medium.

4.2 Morphology Analysis

The morphology of bacterial cellulose was verified by scanning electron microscopy technique (SEM), which was conducted on a JEOL JSM-5200 with an acceleration voltage of 15 kV, magnification in the range of 10,000-15,000 times. All of samples were dried by freeze-dried technique before morphology testing. SEM micrographs of freeze-dried native bacterial cellulose at different magnification (Figure 4.2 (a) and (b)) show three dimensional non-woven nanofibrils with many void spaces among nanofibrils network. The leather-like pellicle consists of overlapping and inter-twisted cellulose ribbons, forming parallel but disorganized planes. The direct measurement indicated that the nanofibrils size is in the range of nanoscale (50 to 100 nm).

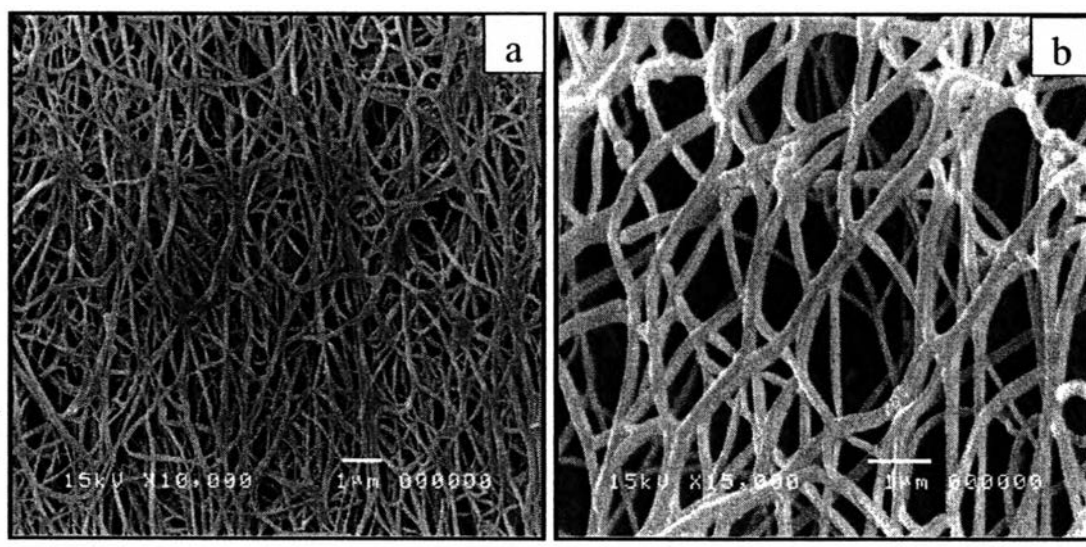

Figure 4.2 SEM micrographs of bacterial cellulose at different magnification : (a) ×10,000 and (b) ×15,000.

Investigation of the texture of bacterial cellulose hydro-gel has shown that a surface layer built on the interface between the culture medium broth and the air shows the pellicle surface clearly. There are three layers on the bacterial cellulose hydro-gel as shown in Figure 4.3 It was found that bacterial cellulose nano-fibrils were very dense on surface layer when comparing with another layer. It is due to the

growth of *Acetobactor Xylinum,* which is aerobic micro-organism, is quit well at the oxygen-rich air-liquid interface.

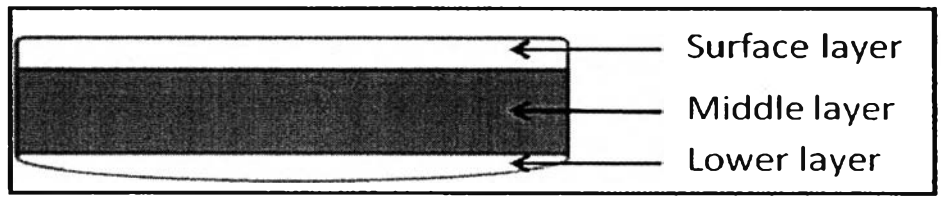

Figure 4.3 Representation of bacterial cellulose layers inside the pellicle.

The micrographs of freeze-dried bacterial cellulose incorporated with polyaniline synthesized by using different amount of aniline monomer monitored by SEM are presented in Figure 4.4. The SEM micrographs indicate that polyaniline can be uniformly deposited on the surface of bacterial cellulose nanofibrils and the thickness of polyaniline particles deposition on bacterial cellulose nanofibrils increased with the amount of aniline monomer, which was used to synthesized polyaniline. There are two reasons for the completely deposition of polyaniline on the surface of bacterial cellulose including; (a) aniline monomer penetrated into bacterial cellulose hydro-gel by using sonication technique and then it was polymerized to polyaniline and deposited on bacterial cellulose nano-fibril and (b) the strong hydrogen bond interaction between polyaniline and bacterial cellulose.

Figure 4.5 shows the SEM micrographs of bacterial cellulose containing both polyaniline, which was synthesized by using 30 %wt of aniline monomer, and magnetite particle (Fe_3O_4) with different in initial concentration of iron precursors (Fe^{2+} and Fe^{3+}). From the SEM micrographs, the completeness of the coating can be seen.

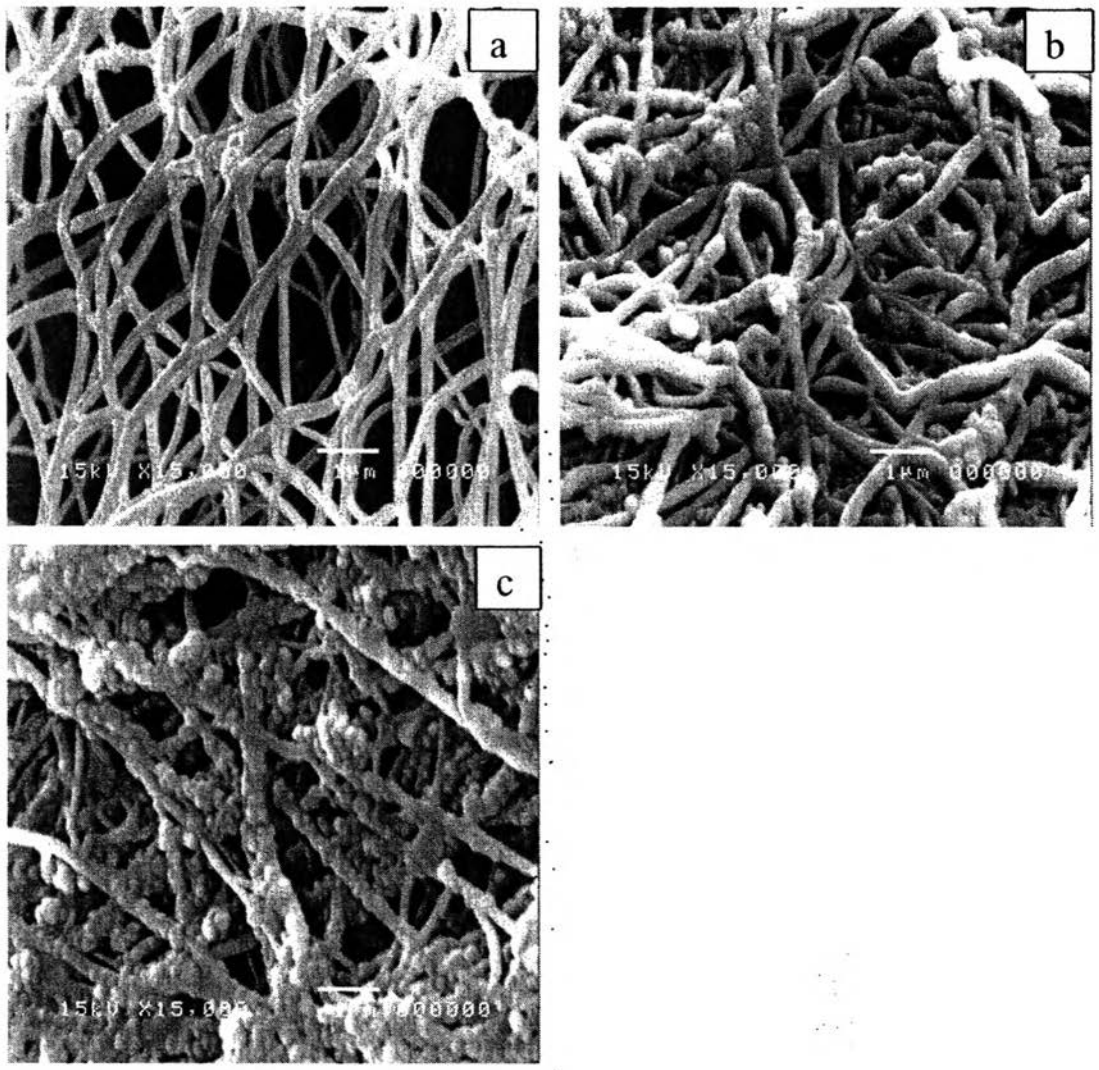

Figure 4.4 SEM micrographs (×15,000) of freeze-dried bacterial cellulose incorporated with PANI synthesized by using different amount of aniline monomer; (a) 0%wt, (b) 15%wt and (c) 30%wt.

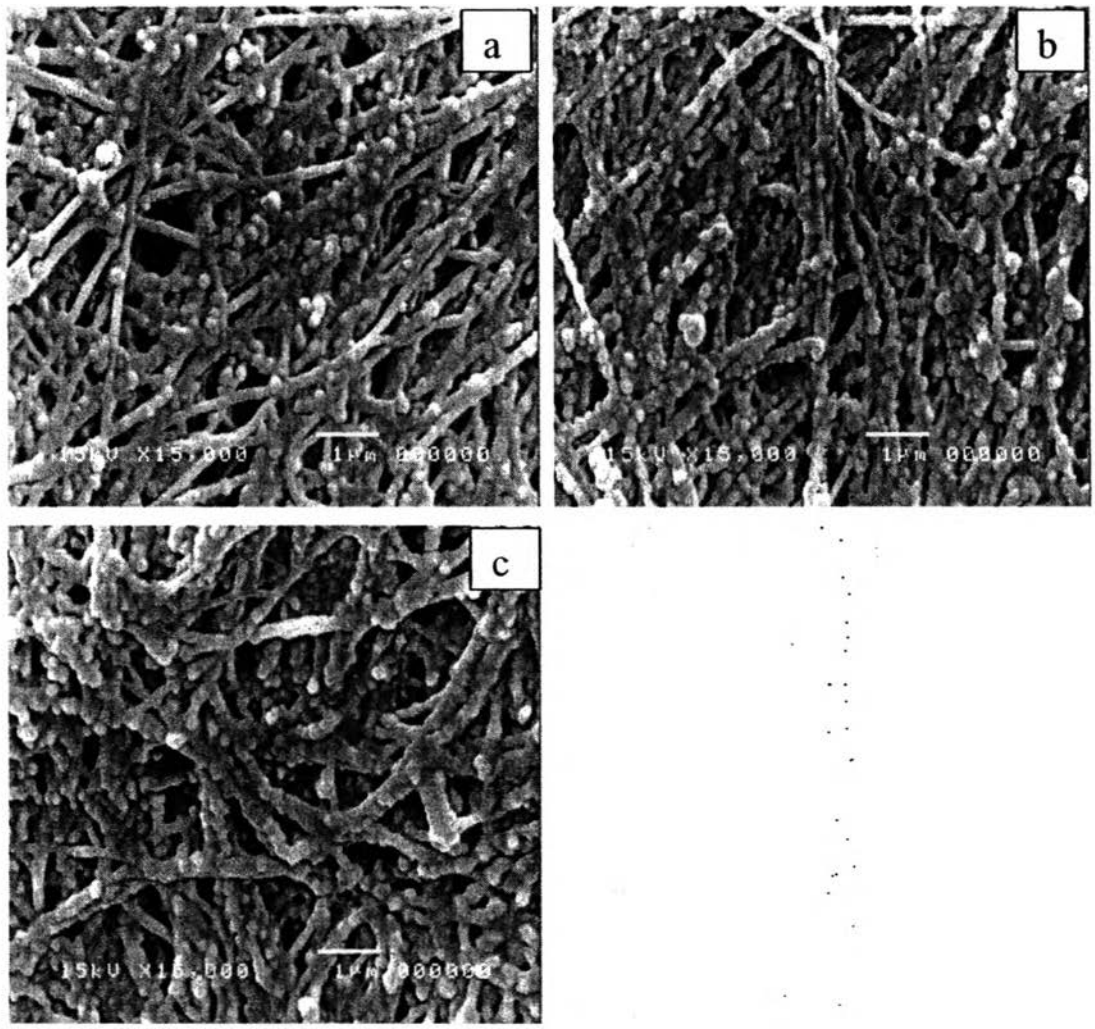

Figure 4.5 SEM micrographs (×15,000) of freeze-dried BC incorporated with different initial concentration of iron precursors; (a) 0.01 M, (b) 0.05 M and (c) 0.10 M. and coated with PANI synthesized by using 30% wt aniline monomer.

4.3 Chemical Structure Analysis

The FTIR spectra of bacterial cellulose (a), polyaniline (b), and bacterial cellulose containing polyaniline (c) are shown in Figure 4.6. The characteristic broad band for O-H group of pure bacterial cellulose appears at 3,410 and 2,900 cm^{-1} due to a symmetrically stretching vibration of C–H in pyranose ring. A broad band around 1,062 cm^{-1} and peak at 1,422 cm^{-1} are attributed to the –C–O–C– and CH_2 of pyranose ring symmetric scissoring respectively. The typical feature in the characteristic peak of pure polyaniline appears at 1,583, 1,497, 1,303, 1,152, and 823 cm^{-1}. The specific wavenumber of FT-IR signals with the possible functional groups are summerized in Table 4.1. The characteristic peaks of both pure bacterial cellulose (2894 and 1407 cm^{-1}) and pure polyaniline (1562, 1480, and 1297 cm^{-1}) have been present on the spectrum of bacterial cellulose containing polyaniline. As the FT-IR spectra results, it can confirm that polyaniline can incorporate into bacterial cellulose.

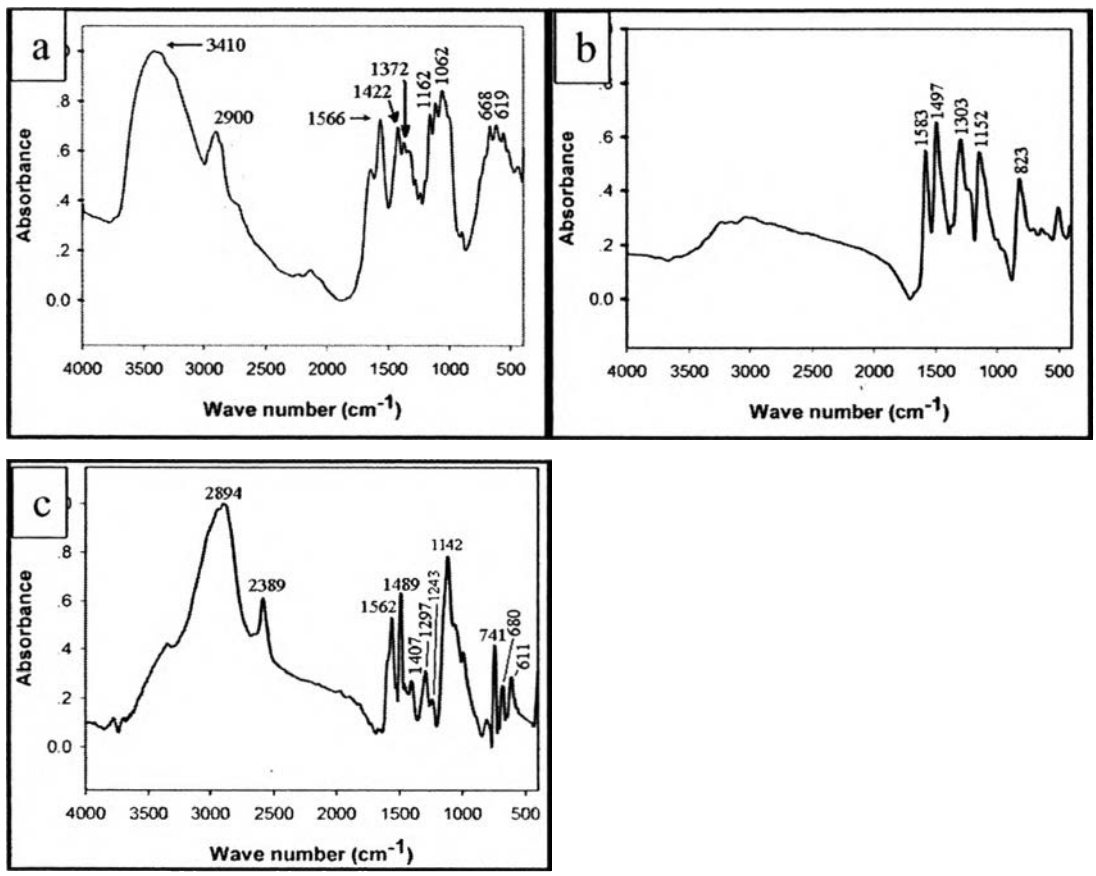

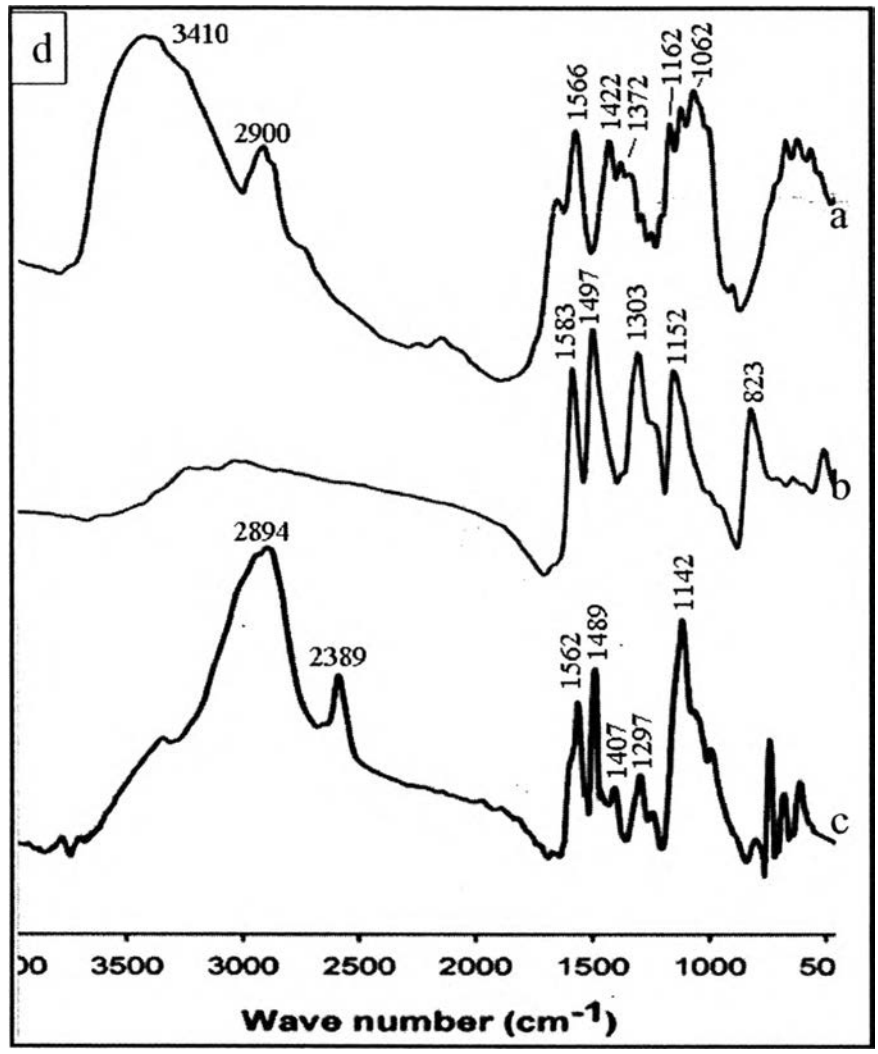

Figure 4.6 FTIR spectra of (a) bacterial cellulose, (b) polyaniline, and (c) bacterial cellulose containing polyaniline and (d) comparison all of samples.

Table 4.1 Main functional groups of all samples

Material	Wave number(cm^{-1})	Functional groups
Polyaniline	1,583	C=C stretching of the quinoid ring
	1,497	C=C stretching of the benzenoid ring
	1,303	C—N stretching of the aromatic secondary amines
	1,152	Vibrational band of N=Q=N stretching (Q representing the quinoid ring)
	823	Out-of plane bending vibration of C—H in the 1, 4-disubstituted benzene ring
Bacterial cellulose	3,410	O-H stretching out of plane deformation
	2,900	CH_2 of pyranose ring symmetric scissoring
	1,422	CH_2 of pyranose ring symmetric scissoring
	1,372	C-H wagging of CH_2 unit
	1,162	-C-O-C- stretching in cyclic ether
	1,062	C-OH stretching
	700-600	C-OH out of plane deformation
Bacterial cellulose containing polyaniline	2,894	CH_2 of pyranose ring symmetric scissoring
	1,562	C=C stretching of the quinoid ring
	1,489	C=C stretching of the benzenoid ring
	1,407	CH_2 of pyranose ring symmetric scissoring
	1,297	C—N stretching of the aromatic secondary amines

4.4 Thermal Stability Study

In the part I, the thermal stability of bacterial cellulose containing polyaniline, was investigated by themogravimetric dynamic temperature analyser (TG-DTA), which was carried out under the condition of nitrogen flow and a heating rate of 10 °C/min. For comparison, the TG-DTA curve of pure bacterial cellulose (a), pure polyaniline (b) and bacterial cellulose containing polyaniline (c) are shown in Figure 4.7. The TG-DTA curve of pure bacterial cellulose indicates that massive weight loss occurred in one step at 180 °C. This result is related to the absence of intermolecular hydrogen bond of bacterial cellulose. It leads to the changing from bacterial cellulose macromolecules into smaller ones. There are three steps of weight loss occurred in TG-DTA curve of polyaniline. The first step of weight loss starting at 80-90 °C is attributed to the removal of moisture present in the polyaniline. The second step of weight loss occuring in between 200-300 °C is may be due to the evaporation of doping agent (HCl). And the weight loss coresponding to the final step at 450-550 °C is mainly attributed to thermal decomposition of polyaniline. For bacterial cellulose containing polyaniline, also there are three steps of weight loss appeared in TG-DTA curve. The first step of weight loss starting at 80-90 °C is attributed to the removal of moisture present in it. The second step of weight loss occuring in between 200-300 °C, there are two reasons for supporting. One is due to the decomposition of bacterial cellulose and another one is due to the evaporation of doping agent (HCl). And the weight loss coresponding to the final step at 450-550 °C is mainly attributed to thermal decomposition of polyaniline. The TG-DTA curve of the series of bacterial cellulose containing polyaniline are shown in Figure 4.8. It is found that there is no remarkable change in thermal behavior and thermal stability in all of incorporated polyaniline, which was polymerized from different amount of aniline monomer. It is explained that polyaniline in bacterial cellulose in all conditions is very small amount so the differrence in TG-DTA curves is not shown.

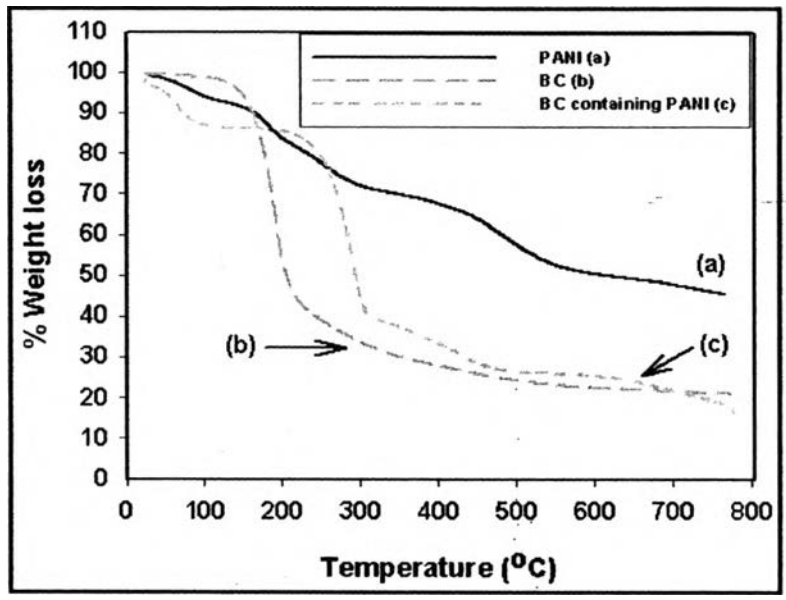

Figure 4.7 TG-DTA curves of (a) polyaniline, (b) bacterial cellulose, and (c) bacterial cellulose containing polyaniline.

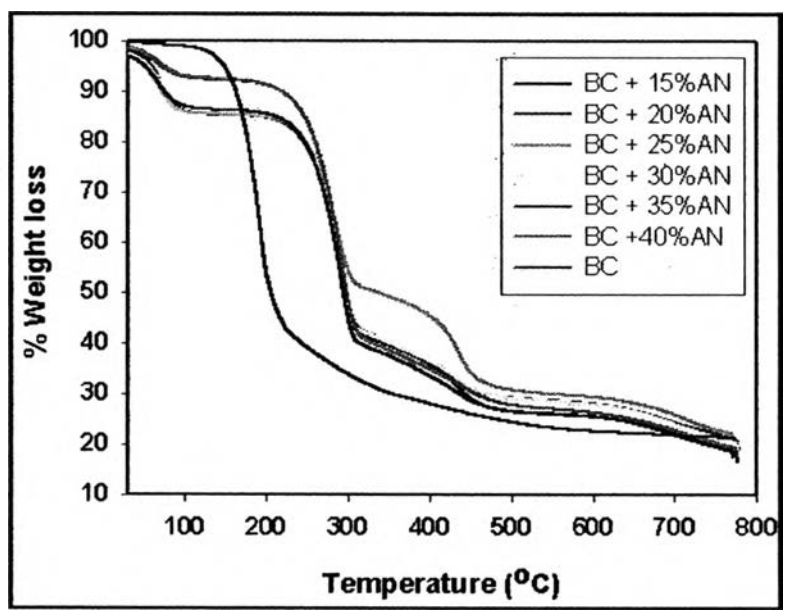

Figure 4.8 TG-DTA curves of pure bacterial cellulose and the series of bacterial cellulose containing polyaniline.

In the part II, the thermal stability of bacterial cellulose sheets containing magnetite particles (Fe_3O_4), was also investigated by themogravimetric dynamic

temperature analyser (TG-DTA), which was carried out under the condition of nitrogen flow and a heating rate of 10 °C/min. Figure 4.9 shows the TG-DTA curves for the all bacterial cellulose containing magnetite particles (Fe_3O_4) at different initial concentration of iron precursors (Fe^{2+} and Fe^{3+}), which consist of 0.01, 0.05, 0.10 and 0.20 M. The TG-DTA curve of pure bacterial cellulose indicates that massive weight loss occurred in one step at 180 °C. This result was related to the absence of intermolecular hydrogen bond of bacterial cellulose. The TG-DTA curves of all the samples except the pure bacterial cellulose (a) indicate that they undergo two main stages in the temperature ranges of 100–150 °C and 250–300 °C respectively. The first weight loss (100–150 °C) is associated with the loss of moisture. After that there is a significant weight loss from 250 °C to 300 °C, corresponding to the decomposition of the bacterial cellulose. However, significant weight loss of decomposition of Fe_3O_4 can not be observed due to the decomposition temperature of Fe_3O_4 is higher than 800 °C. The onset temperature of degradation of pure bacterial cellulose is observed at 180 °C, which is lower 70 °C than the bacterial cellulose containing Fe_3O_4. In this sense, it indicates that the thermal stability of bacterial cellulose containing Fe_3O_4 is increased than pure bacterial cellulose. It is because Fe_3O_4 particles, which deposited on the surface of bacterial cellulose, acted as safeguard for bacterial cellulose. The char yield continuously increases with increasing the initial concentration of iron precursors as summarized in Table 4.2. High amount of iron precursors can penetrate into bacterial cellulose hydro-gel when used high concentration, therefore, after the precipitation with ammonia gas in order to form magnetite particles, higher amount of magnetite particles was produced and deposited on the surface of bacterial cellulose comparing with low initial precursors concentration.

Table 4.2 Char yield content in bacterial cellulose containing Fe_3O_4 at different initial concentration of iron precursors.

Initial concentration of iron precursors (mol/l)	Used precusors (g)		% Char yield
	$FeSO_4 \cdot 7H_2O$	$FeCl_3 \cdot 6H_2O$	
0.01	0.459	0.895	22
0.05	2.294	4.477	34
0.10	4.587	8.953	47
0.20	9.174	17.906	62

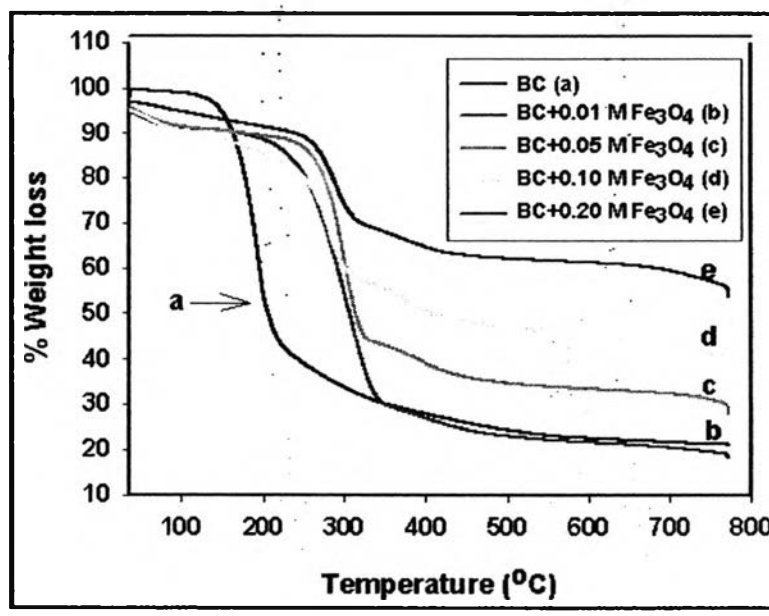

Figure 4.9 TG-DTA curves of pure bacterial cellulose and the series of bacterial cellulose containing magnetite particles (Fe_3O_4).

4.5 Electrical Properties Study

4.5.1 Effect of Incorporated Polyaniline with Synthesized by Using Different Amount of Aniline Monomer in Doped and Un-doped State

It is generally accepted that polyaniline doped by protonic acids displays more excellent conductivity than the ones un-doped. The electrical conductivity of polyaniline highly depended on the types of acids used. Therefore, in this work, only HCl was used to dope polyaniline in order to study only the effect of aniline monomer content, which was polymerized to polyaniline and incorporated into bacterial cellulose nanofibrils, on the electrical conductivity of the bacterial cellulose containing polyaniline. In part I, the effect of aniline monomer which was used to synthesized polyaniline and the relative humidity on the electrical conductivity of bacterial cellulose sheets containing polyaniline were investigated. Table 4.3 lists the effects of the polyaniline with synthesized by using different amount of aniline monomer, which was incorporated into bacterial cellulose sheets, on the electrical conductivity of bacterial cellulose containing polyaniline in both un-doped and doped states and also Figure 4.10 shows tendency of electrical conductivity on the polyaniline with synthesized by using different amount of aniline monomer. The doped state was carried out by using 50 ml of 0.48 M HCl as doping agent for one sheet of bacterial cellulose containing polyaniline. The electrical conductivity of doped bacterial cellulose containing polyaniline increases from 2.29 to 6.17 S/cm with the increasing in amount of aniline monomer, which was used to synthesize polyaniline, from 15 to 30%wt. It could be explained that in the excessive acids region, a large number of polyaniline were synthesized and deposited on the surface of bacterial cellulose nanofibrils because of the strong hydrogen bond interaction between polyaniline and hydrogen groups of bacterial cellulose. The proposed formation mechanism of hydrogen bond between polyaniline and bacterial cellulose is shown in Figure 4.11. There are two possible ways for hydrogen bond formation: the first one is the interaction between nitrogen from polyaniline and hydrogen from bacterial cellulose, and another one is the interaction between hydrogen from polyaniline and oxygen from bacterial cellulose. The percolation threshold was observed when aniline monomer, which was used to synthesized polyaniline,

increases from 30% to 40%wt. It could be explained that there are the limitation for deposition of polyaniline on the surface of bacterial cellulose nanofibrils although bacterial cellulose nanofibrils have high surface area. For un-doped state of bacterial cellulose containing polyaniline sheets, which were carried out by immersing one bacterial cellulose sheet containing polyaniline into 50 ml of 0.48 M NaOH for 12 h, the electrial conductivity is less than the doped state of bacterial cellulose sheets containing polyaniline about 1,000 times is due to the general property of emeraldine base. The electrical conductivity in any system is proportional to the density of charge carriers. If no presence of doping agent, the chemical structure of polyaniline is usual conjugated system as shown in Figure 4.12, there is no charge carriers, results in low electrical conductivity.

Table 4.3 Effects of the polyaniline with synthesized by using different amount of aniline monomer on the electrical conductivity

% Aniline monomer	Electrical conductivity(S/cm)			
	Doped state		Un-doped state	
	Average	SD	Average	SD
0	1.65×10^{-4}	5.18×10^{-5}	1.65×10^{-4}	5.18×10^{-5}
15	2.29	5.17×10^{-1}	4.53×10^{-4}	1.78×10^{-4}
20	3.16	6.89×10^{-1}	4.89×10^{-4}	2.34×10^{-4}
25	4.16	1.20	5.17×10^{-4}	2.54×10^{-4}
30	6.17	1.84	5.77×10^{-4}	1.53×10^{-4}
35	5.75	2.12	5.37×10^{-4}	1.81×10^{-4}
40	5.73	8.63×10^{-1}	5.32×10^{-4}	2.01×10^{-4}

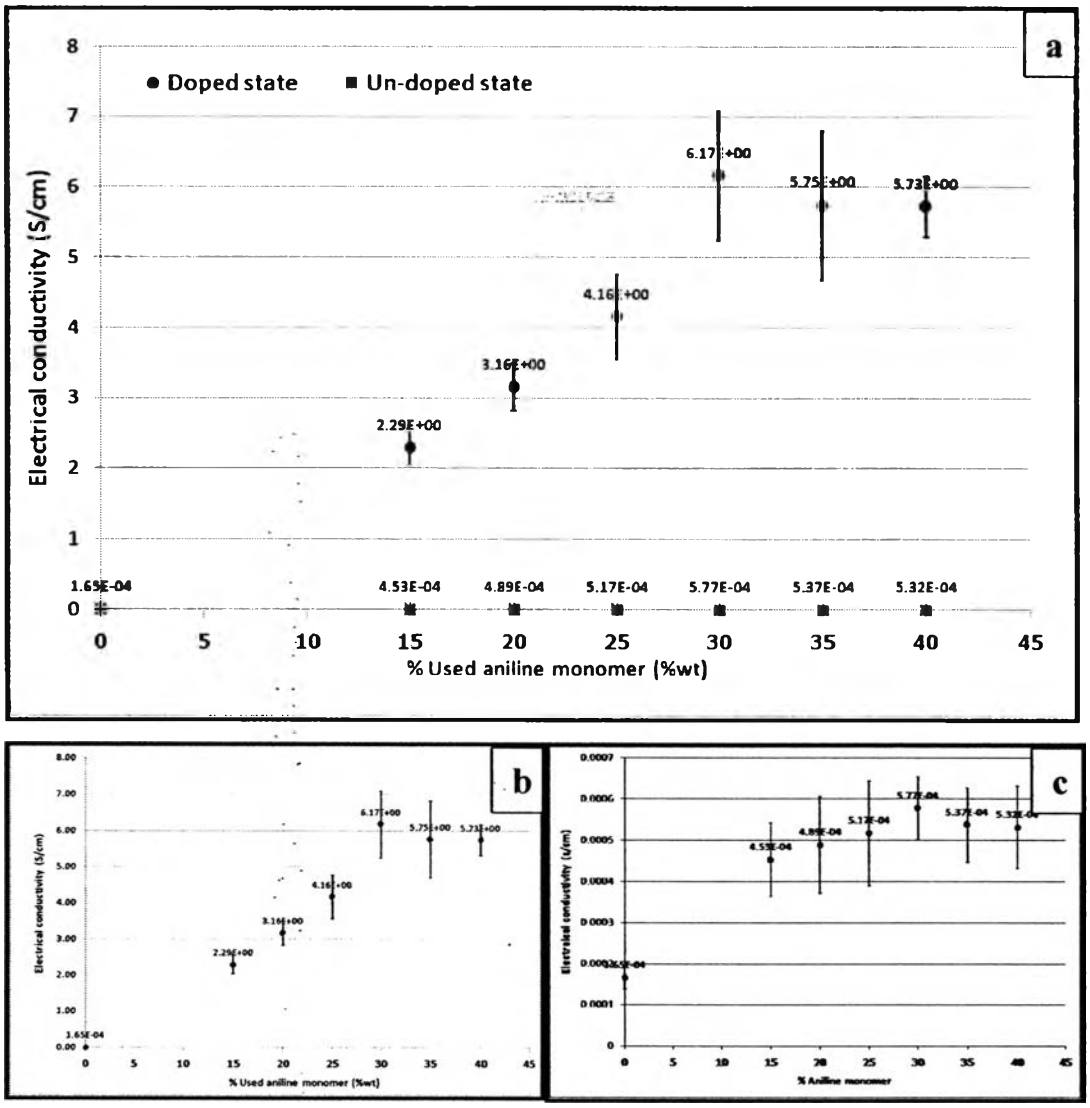

Figure 4.10 Electrical conductivity of BC containing PANI as a function of % aniline monomer which was used to polymerize PANI; (a) in both doped and un-doped state, (b) doped state, and (c) un-doped state.

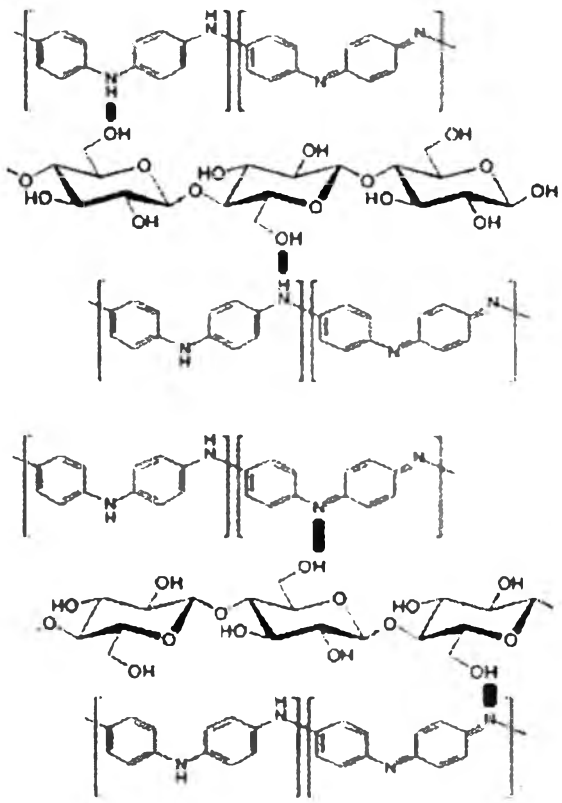

Figure 4.11 Two possible ways for hydrogen bond formation between polyaniline and bacterial cellulose.

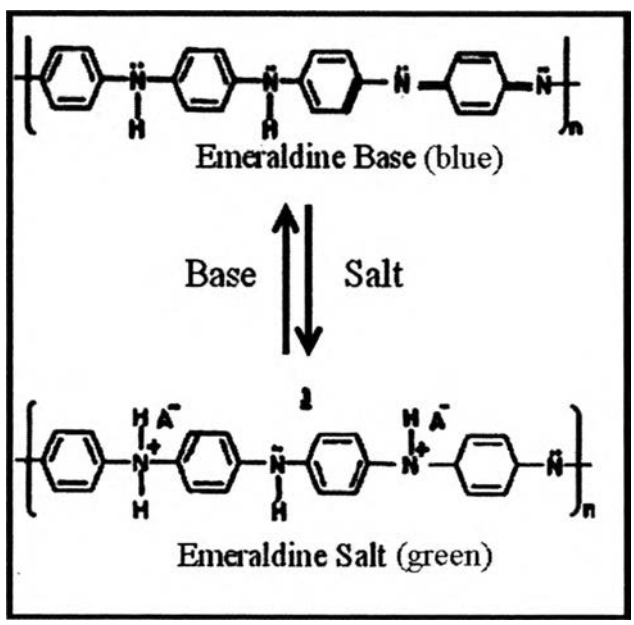

Figure 4.12 Chemical structure of doped and un-doped state.

4.5.2 Effect of Impregnation Time

Table 4.4 lists the effects of the impregnation time on the electrical conductvity of bacterial cellulose sheets containing polyaniline. All of samples were prepared by oncorporating of polyaniline with synthesized by using 30 %wt of aniline monomer in bacterial cellulose sheets and doped with 50 ml of 0.48 M HCl per one sheet of bacterial cellulose containing polyaniline. The results was analyzed in term of statistical by using SPSS program under 95% confidence and indicated that the electrical conductivity increased with increasing of the impregnation time from 30 minute to 6 hour. Although, very long impregnetion time (3-6 h) was used in order to increase the penetration efficiency, the electriacal conductivity did not much increase. Therefore, only 30 minute of imprenation time is appropriate time for preparing in all of samples because this time can provide reasonable electrical conductivity by using less time.

Table 4.4 Effect of impregnation time on the electrical conductivity

Impregnation time (h)	Electrical conductivity(S/cm)	
	Average	SD
0.5	6.17	1.84
3	7.74	3.08
6	8.45	4.37

4.5.3 Effect of Relative Humidity

Three salt were used for making a low, medium, and high humidity range. These are LiCl (11.3%), K_2CO_3 (43.2%), and NaCl (75.3%) relative humidities The experiments was done to stydy the effect of relative humidity on the electrical conductivity of bacterial cellulose sheets containing polyaniline. One bacterial cellulose sheet containing polyaniline was doped in 50 ml of 0.48 M-HCl. for 12 hours. The results were analyzed in term of statistical by using SPSS program under 95% confidence and tabulated in Table 4.5. It is found that the increasing of electrical conductivity of bacterial cellulose sheets containing polyaniline with increasing in relative humidity. It can be explained on the basis of proton exchange mechanism. In presence of water molecule, proton can easily transfer. Therefore, the role of water is

importance for this mechanism. The reactions in presence of humidity may be expected to result in the variation of electrical conductivity of bacterial cellulose sheets containing polyaniline.

Table 4.5 Effect of relative humidity on the electrical conductivity

Type of salt	Relative humidity	Electrical conductivity(S/cm)	
		Average	SD
LiCl	11.3	2.02	0.61
K_2CO_3	43.2	4.80	2.65
NaCl	75.3	7.06	2.78

4.5.4 Effect of Initial Concentraion of Iron precursors (Fe^{2+} and Fe^{3+})

In partII, a standard two–point probe technique was used to measure the surface conductivity of bacterial cellulose sheets containing Fe_3O_4 and containing both of Fe_3O_4 and polyaniline. For the electrical conductivity of bacterial cellulose containing magnetite particles (Fe_3O_4) at different initial concentration of iron precursors (Fe^{2+} and Fe^{3+}), which consist of 0.01, 0.05, 0.10 and 0.20 M, were analyzed in term of statistical by using SPSS program under 95% confidence and tabulated in Table 4.6 and shown tendency in Figure 4.13. It is found that bacterial cellulose sheets containing Fe_3O_4 do not show the electrical properties, which has the electrical condctivity in magnetude of 10^{-4}. It is due to intrinsic properties of Fe_3O_4 particles, which are small particles having large exposed surface area and are prone to oxidation, and therefore the particles have a resistance. For bacterial cellulose sheets containing Fe_3O_4 and coated with polyaniline, the samples were prepare by using aniline monomer 30 %wt of bacterial cellulose sheets containing Fe_3O_4 at differrent initial concentraion of iron precursors. And it is found that when the bacterial cellulose sheets containing Fe_3O_4 were coated with polyaniline, the electrical conductivity was significant increased about 2000 times. It can be explained that the coating of polyaniline bacterial cellulose sheets containing Fe_3O_4 can induce the opportunity to add electrical conductivity to polyaniline bacterial cellulose sheets containing Fe_3O_4 because polyailine shows its intrinsic preperties.

Table 4.6 The electrical conductivity of bacterial cellulose sheets containing Fe_3O_4 particles with and without polyaniline

Initial concentration of iron precursors (mol/l)	Electrical conductivity (S/cm)			
	With out PANI		With PANI	
	Average	SD	Average	SD
0	1.65×10^{-4}	5.18×10^{-5}	6.17	1.84
0.01	4.38×10^{-4}	2.15×10^{-4}	1.15	0.21
0.05	5.75×10^{-4}	2.98×10^{-4}	1.21	0.42
0.10	5.06×10^{-4}	1.84×10^{-4}	1.23	0.36
0.20	6.58×10^{-4}	2.81×10^{-4}	1.29	0.58

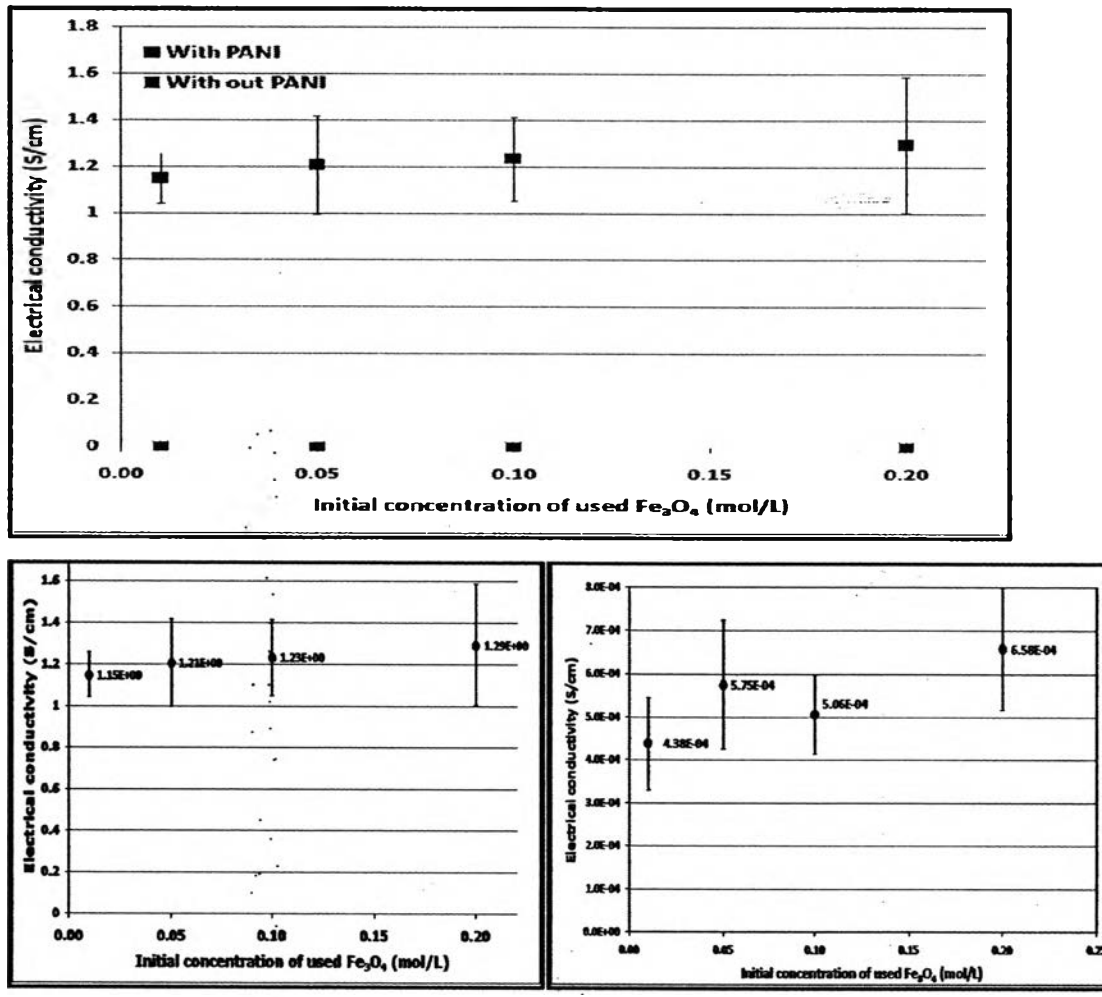

Figure 4.13 Effect of initial used iron ions (Fe^{2+} and Fe^{3+}) concentration on the electrical conductivity; (a) in both with and without polyaniline, (b) with polyaniline, and (c) without polyaniline.

4.6 Magnetic Properties Studies

The magnetic properties of all samples, which consist of bacterial cellulose containing only Fe_3O_4 and both of Fe_3O_4 and polyaniline, such as specific magnetization at saturation, M_s, and the coercive force, H_c reported in Table 4.7 were calculated from their hysteresis loops obtained for each sample using a vibrating sample magnetometer. Figure 4.14 shows the magnetic properties of the samples with different in initial concentration of iron precursors (Fe^{2+} and Fe^{3+}). It is evident that there is a linear relationship between the saturated magnetization and the initial concentration of iron precursors. A higher initial concentration of iron precursors has greater the saturated magnetization (M_s). The samples of bacterial cellulose containing only Fe_3O_4 show saturated magnetization of 3.14 to18.38 $emug^{-1}$ and show very small hysteresis loops. Coercive fields for all of samples are very low; H_c =~ 59.51–82.26 Oe. A coercive field as low as this is ideal for application in electromagnetic shielding (Aaron C. et al., 2009). In addition, magnetic properties of bacterial cellulose sheets containing both Fe_3O_4 and polyaniline were also investigated and found that the saturated magnetization is lower than the case of bacterial cellulose containing only Fe_3O_4. It is due to Fe_3O_4, which is the main component that shows the magnetic properties, was cover by polyaniline, therefore some interference from polyaniline can affect on the magnetic properties, as result in the decreasing of magnetic properties. The hysteresis loops of bacterial cellulose sheets containing both Fe_3O_4 and polyaniline are shown in Figure 4.15.

Table 4.7 Magnetic properties of the samples in all conditions

Initial concentration of iron precursors (mol/l)	Electrical conductivity (S/cm)			
	With out PANI		With PANI	
	M_s (emu/g)	H_c (Oe)	M_s (emu/g)	H_c (Oe)
0.05	3.14	59.51	2.47E-01	74.75
0.10	5.21	77.74	1.23	75.38
0.20	18.38	82.26	5.38	85.44

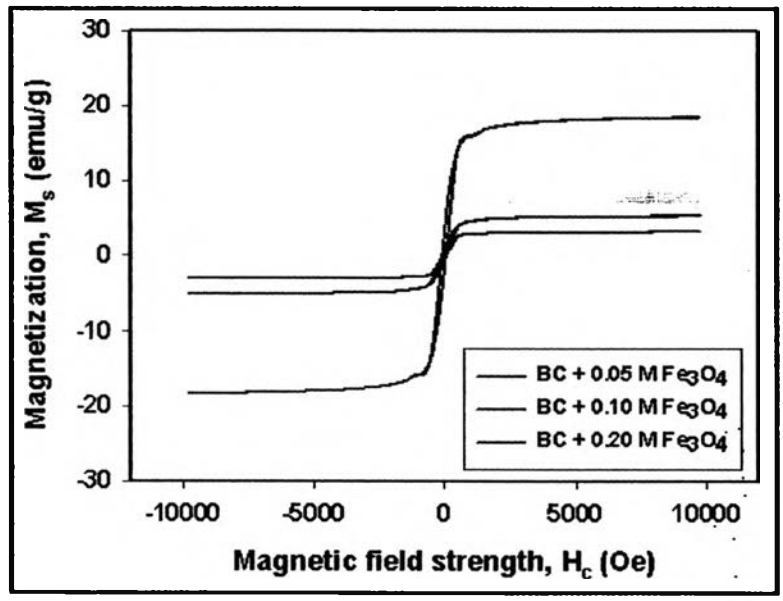

Figure 4.14 Magnetic hysteresis loop of bacterial cellulose sheets containing Fe_3O_4

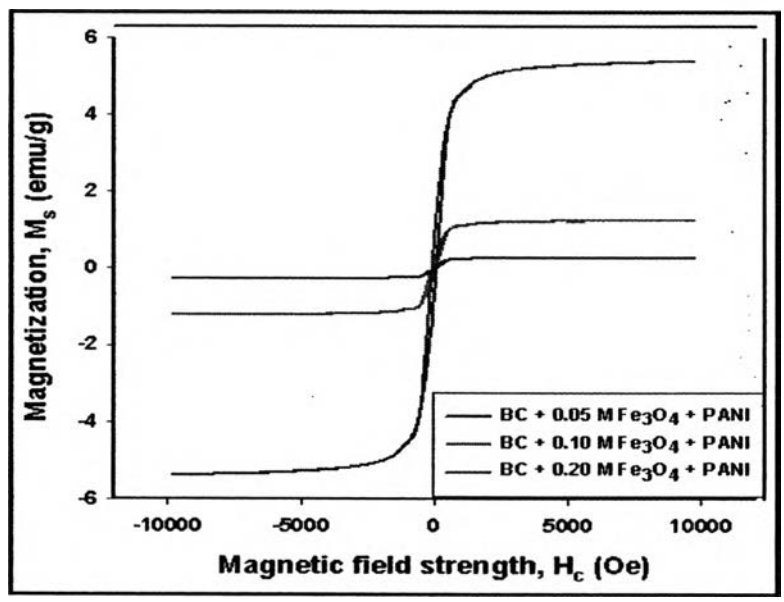

Figure 4.15 Magnetic hysteresis loop of bacterial cellulose sheets containing Fe_3O_4 and polyaniline.

4.7 Electromechanical Actuation Study

Electromechanical actuation of bacterial cellulose film containing polyaniline was investigated in term of bending deformation in transparent cell-box with a pair of parallel copper electrode plates, nuetral plate and anode plate, which were coupled with high DC voltage under applied electric field in range from 0-750 V/mm. The film sample was synthesized by using 30 %wt of aniline monomer and doped with 0.48 M HCl for 12 hours. The video digital camera was used to record the bending deformation and the photographs are shown in Figure 4.16. It was found that the film of bacterial cellulose containing polyaniline bent toward the nuetral plate, which was considered as a cathode side under applied electric field. The reason of bending of film to nuetral plate comes from polyaniline, which exists in the conducting state that has positive charge along the chain, so it is possible to contribute in the bending to nuetral plate, which was considered as a cathode side under applied electric field resulting from Coulomb interaction. On the other hand, applied energy or electric field can induce the emitting of electron on the chain of polyaniline, which is one behavior of conductive polymer, so it is the other one reason for bending of the film to nuetral plate. In this study, deflection distance and deflection angle were investigated as the function of applied electric field. It was found that the bending deformation of this film started at applied electric field of 400 V/mm and the bending deformation increased with the increasing of applied electric field as shown in Figure 4.17 and 4.18.

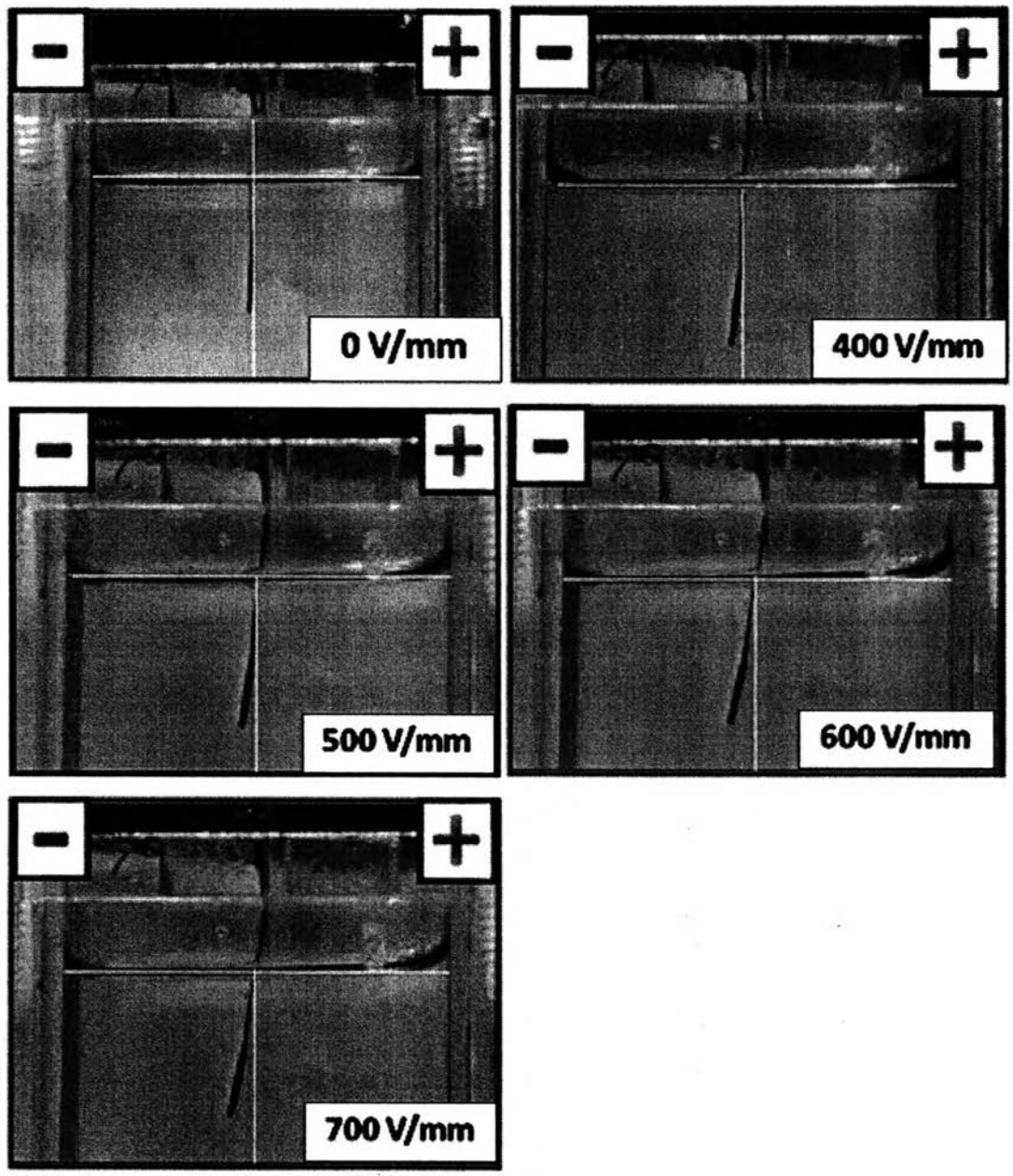

Figure 4.16 Captured digital camera images of bending of bacterial cellulose film containing polyaniline

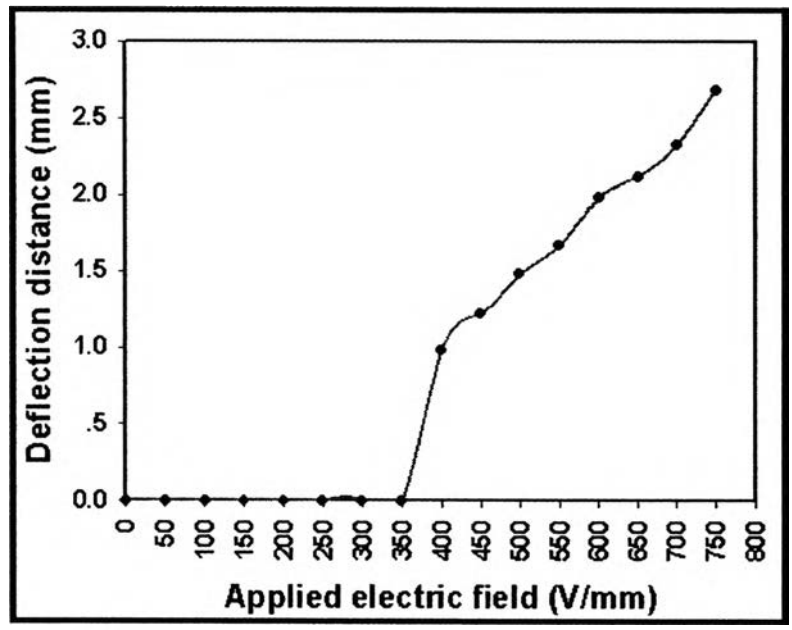

Figure 4.17 Deflection distance of bacterial cellulose film containing polyaniline as a function of applied electric field

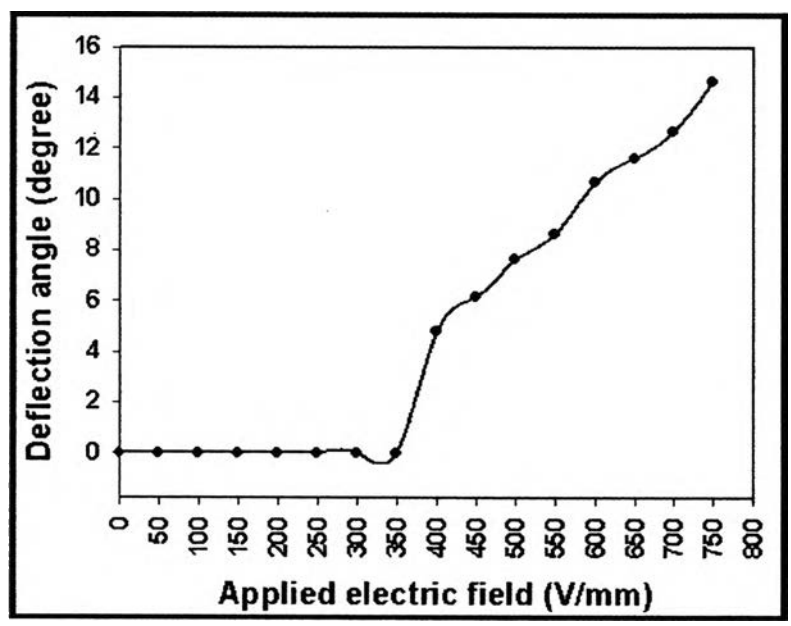

Figure 4.18 Deflection angle of bacterial cellulose film containing polyaniline as a function of applied electric field